

Stats for Live
Cells

Huckemann

Image
Enhancement

Drift Model

Asymptotics

Simulations

Application

Stem Cells

Polarization

SiZer

WiZer

Biomechanics

Discussion

References

References

Some Statistics for Live Biological Cells

Drift estimation in sparse sequential dynamic imaging and circular scale space theory

Stephan F. Huckemann

University of Göttingen,
Felix Bernstein Institute for Mathematical Statistics in the Biosciences

Feb. 12, 2016

Mathematical Statistics and Inverse Problems
February 8-12, 2016, CIRM



supported by the

Niedersachsen Vorab of the
Volkswagen Foundation



Contributors

Institute for Mathematical Stochastics Göttingen Jörn Dannemann, Benjamin Eltzner, Carsten Gottschlich, Alexander Hartmann, Axel Munk, Ina Schachtschneider and Max Sommerfeld

Laser Laboratory Göttingen Alexander Egner, Claudia Geisler and Oskar Laitenberger

Physics III/Biophysics, Univ. Göttingen Florian Rehfeldt and Carina Wollnik

School of Mathematical Sciences, Univ. Nottingham Kwang-Rae Kim



Supported by DFG SFB 755 “Nanoscale Photonic Imaging”,
the Niedersachsen Vorab of the Volkswagen Stiftung and
the SAMSI 13/14 Program LDHD

Introduction

- Assessing micro and nano structures in living cells,
- e.g. the cytoskeleton,
- consisting of actin-myosin bundles, intermediate filaments and microtubules.
- Statistical tasks
 - feature extraction
 - feature analysis

Introduction

- Assessing micro and nano structures in living cells,
- e.g. the cytoskeleton,
- consisting of actin-myosin bundles, intermediate filaments and microtubules.
- Statistical tasks
 - feature extraction
 - feature analysis
- leading to
 - ① a stochastic deconvolution model with asymptotics in the sparsity for image enhancement and
 - ② the circular or Wrapped SiZer feature analysis with application to stem cell diversification.

Image Enhancement for the Microtubules Skeleton

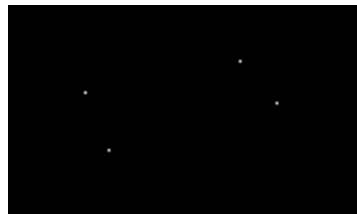
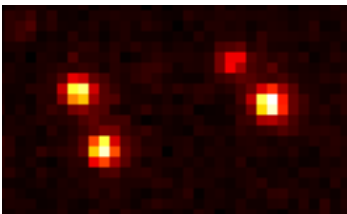
- Objective: fine *in vivo* structure resolution
 - structural cell network
 - in mitotic spindle
 - cell division
 - cancer treatment
 - here: β -tubulin
- Method: fluorescence imaging (visible light)
- Width ≈ 25 nm
- Challenge: Abbe (1873) diffraction barrier

$$d \approx \frac{\lambda}{2 \text{ numerical aperture}} \geq 200 \text{ nm}$$

Overcoming Abbe's Limit

- Several methods developed in the last decades, 4PI, STED, SMS, etc., cf. Hell (2007)
- SMS = **single marker switching** (also known as PALM by Betzig et al. (2006), STORM by Rust et al. (2006), PALMIRA by Egner et al. (2007)):
 - ① One laserbeam provides energy for photon emission,
 - ② another low energy laserbeam excites (ideally) a single molecule (switch on) which then emits photons for a while (until it switches itself off),
 - ③ confocally record photon origin,
 - ④ estimate with high precision center of a Gaussian,
 - ⑤ GoTo 2
- precision \sim number of photons
- \rightarrow waiting time
- \rightarrow **drift blur**.

Single Molecule Localization



Left: ≈ 140 nm resolution.
(individual protein ≈ 2 nm)

Right ≈ 20 nm resolution

PALMIRA (Egner et al. (2007)): Photoactivated localization microscopy with independently running acquistion:

- Acquistion time \approx few minutes,
- to account for drift effects an always (over)shining *bead* is introduced.
- **Can we do without a bead?**

Challenge

- Classical drift (motion) estimation assumes to observe the (noisy) **entire image** each time point
- Here: only noisy **few image pixel** observations per time point

First and last single images of PALMIRA data



Challenge and Plan

- Classical drift (motion) estimation assumes to observe the (noisy) **entire image** each time point
- Here: only noisy **few image pixel** observations per time point
- Geisler et al. (2012) introduced a general model free practical method
- Here: Gaussian (approximation) model and statistical features via **Fourier methods**
 - linearly superimpose image in the Fourier domain
 - linear drift becomes shift in the Fourier domain
- Novel asymptotics:
 - $\#\{\text{time points}\} \nearrow$
 - image sparsity \nearrow

A Few Observation's Drift Model

The few observation's regression model

$$y_{j_l^t, t} = f(x_{j_l^t} - \delta_t) + \sigma_{j_l^t, t} \epsilon_{j_l^t, t}, \quad \epsilon_{j_l^t, t} \stackrel{i.i.d.}{\sim} \mathcal{N}(0, 1), \quad \sigma_{j_l^t, t} > 0$$

with

- f : unknown true image intensity,
- observed image intensities $y_{j_l^t, t}$ at
- time points $t \in \mathbb{T} := \{0, \frac{1}{T}, \frac{2}{T}, \dots, \frac{T-1}{T}\}$ ($T > 0$),
- for each t , at few $x_{j_l^t}$ ($l = 1, \dots, n_t \approx \text{constant}$, some binning) locations of n uniform pixel locations $\in [0, 1]^2$
- δ_t : 2D pixel location valued drift,

has the discrete Fourier transform

$$Y_k^t = f_k^t + \frac{\sigma}{\sqrt{n_t}} W_k^t, \quad k \in \mathbb{Z}^2$$

for each t with

- i.i.d. (standard) complex normals W_k^t .

Novel Asymptotics

The Fourier model:

$$Y_k^t = f_k^t + \frac{\sigma}{\sqrt{n_t}} W_k^t, \quad k \in \mathbb{Z}^2, \quad t = 0, \frac{1}{T}, \dots, \frac{T-1}{T}$$

where

- n fixed (some binning s.t. n_t fixed, constant and only few single molecules),
- denoting $\sigma/\sqrt{n_t}$ by σ ,
- exploiting the **shift property**:

$$f_k^t = f(\cdot - \delta_t)_k = \underbrace{e^{-2\pi i \langle k, \delta_t \rangle}}_{=: h_k(-\delta_t)} f_k$$

- $T \rightarrow \infty$,

motivates the **sequence model**

$$Y_k^t = h_k(-\delta_t) f_k + \sigma W_k^t, \quad k \in \mathbb{Z}^2, \quad t = 0, \frac{1}{T}, \dots, \frac{T-1}{T}.$$

Semiparametric Estimation

Parametric drift model: $\delta_t = \delta_t^\vartheta$, $\vartheta \in \Theta$ compact $\subset \mathbb{R}^d$

(Sparse) sequence model: $Y_k^t = h_k(-\delta_t^\vartheta) f_k + \sigma W_k^t$

Contrast functionals (empirical, population):

$$\begin{aligned} M_T(\vartheta) &:= \frac{1}{T} \sum_{|k|<\xi_T} \sum_{t \in \mathbb{T}} \left| h_k(\delta_t^\vartheta) Y_k^t - \frac{1}{T} \sum_{t' \in \mathbb{T}} h_k(\delta_t^\vartheta) Y_k^{t'} \right|^2 \\ &= \sum_{|k|<\xi_T} \left(\frac{1}{T} \sum_{t \in \mathbb{T}} \left| h_k(\delta_t^\vartheta) Y_k^t \right|^2 - \left| \frac{1}{T} \sum_{t' \in \mathbb{T}} h_k(\delta_{t'}^\vartheta) Y_k^{t'} \right|^2 \right) \\ &= M_T^0 + \tilde{M}_T(\vartheta) \end{aligned}$$

$$\begin{aligned} M(\vartheta) &:= \sum_{k \in \mathbb{Z}^2} \int_0^1 \left| h_k(\delta_t^\vartheta - \delta_{t'}^{\vartheta_0}) f_k - \int_0^1 h_k(\delta_{t'}^\vartheta - \delta_{t'}^{\vartheta_0}) f_k dt' \right|^2 dt \\ &= \sum_{k \in \mathbb{Z}^2} |f_k|^2 \left(1 - \left| \int_0^1 h_k(\delta_t^\vartheta - \delta_{t'}^{\vartheta_0}) dt \right|^2 \right) = M^0 + \tilde{M}(\vartheta) \end{aligned}$$

Estimators and Assumptions

For given $T > 0$ and choice of $\xi_T > 0$,

- **drift estimator:** $\hat{\vartheta}_T \in \arg \min_{\vartheta \in \Theta} M_T(\vartheta)$
- **image estimator:**

$$\hat{f}_T(x) := \sum_{|k| < \xi_T} \frac{1}{T} \sum_{t \in \mathbb{T}} h_k(\delta_t^{\hat{\vartheta}_T}) Y_k^t e^{2\pi i \langle k, x \rangle}.$$

Assumptions:

- $\delta_t^\vartheta =$ polynomial of fixed degree in t with coefficients determined by $\vartheta \in \Theta$.
- for $\rho = 1$

$$f \in H^\rho([0, 1]^2) := \left\{ f \in L^1([0, 1]^2) : \sum_{k \in \mathbb{Z}^2} (1 + |k|^2)^{\frac{\rho}{2}} |f_k|^2 < \infty \right\}$$

- $\exists k_1, k_2, k'_1, k'_2, k''_1, k''_2, k'''_1, k'''_2 \in \mathbb{Z}$ such that $k_1 k'_2 - k_2 k'_1 \neq 0 \neq k''_1 k'''_2 - k''_2 k'''_1$, have no common divisors and $|f_k| \neq 0 \forall k \in \{(k_1, k_2), (k'_1, k'_2), (k''_1, k''_2), (k'''_1, k'''_2)\}$.

Consistency

Theorem 1

Under the assumptions, if $\xi_T \xrightarrow{T \rightarrow \infty} \infty$ and $\xi_T = o(\sqrt{T})$ then

$\hat{\vartheta}_T \xrightarrow{a.s.} \vartheta_0$ (population minimizer), $\left\| \hat{f}_T - f \right\|_2 \xrightarrow{p} 0$ ($T \rightarrow \infty$).

If even $\xi_T = o(T^{1/4})$ then $\left\| \hat{f}_T - f \right\|_2 \xrightarrow{a.s.} 0$.

Proof.

To see $\hat{\vartheta}_T \xrightarrow{a.s.} \vartheta_0$ show

(1) uniqueness of the constraint minimizer ϑ_0

(2) continuity of $\vartheta \mapsto \tilde{M}(\vartheta)$

(3) $\tilde{M}_T(\vartheta) \xrightarrow{a.s.} \tilde{M}(\vartheta)$ uniformly in ϑ as $T, \xi_T = o(\sqrt{T}) \rightarrow \infty$

Finally show that the order of $\|\hat{f}_T - f\|^2$ is that of

$$\left\| \hat{\vartheta}_T - \vartheta_0 \right\| \frac{1}{\sqrt{T}} \sum_{|k| < \xi_T} |f_k| |k| |G_k^T|$$

Consistency

Theorem 1

Under the assumptions, if $\xi_T \xrightarrow{T \rightarrow \infty} \infty$ and $\xi_T = o(\sqrt{T})$ then

$\hat{\vartheta}_T \xrightarrow{a.s.} \vartheta_0$ (population minimizer), $\left\| \hat{f}_T - f \right\|_2 \xrightarrow{p} 0$ ($T \rightarrow \infty$).

If even $\xi_T = o(T^{1/4})$ then $\left\| \hat{f}_T - f \right\|_2 \xrightarrow{a.s.} 0$.

Proof.

To see $\hat{\vartheta}_T \xrightarrow{a.s.} \vartheta_0$ show

(1) uniqueness of the constraint minimizer ϑ_0

(2) continuity of $\vartheta \mapsto \tilde{M}(\vartheta)$

(3) $\tilde{M}_T(\vartheta) \xrightarrow{a.s.} \tilde{M}(\vartheta)$ uniformly in ϑ as $T, \xi_T = o(\sqrt{T}) \rightarrow \infty$

Finally show that the order of $\|\hat{f}_T - f\|^2$ is that of

$$\left\| \hat{\vartheta}_T - \vartheta_0 \right\| \frac{\xi_T}{\sqrt{T}} \frac{1}{\xi_T} \sum_{|k| < \xi_T} |f_k| |k| |G_k^T|$$

Consistency

Theorem 1

Under the assumptions, if $\xi_T \xrightarrow{T \rightarrow \infty} \infty$ and $\xi_T = o(\sqrt{T})$ then

$\hat{\vartheta}_T \xrightarrow{a.s.} \vartheta_0$ (population minimizer), $\left\| \hat{f}_T - f \right\|_2 \xrightarrow{p} 0$ ($T \rightarrow \infty$).

If even $\xi_T = o(T^{1/4})$ then $\left\| \hat{f}_T - f \right\|_2 \xrightarrow{a.s.} 0$.

Proof.

To see $\hat{\vartheta}_T \xrightarrow{a.s.} \vartheta_0$ show

(1) uniqueness of the constraint minimizer ϑ_0

(2) continuity of $\vartheta \mapsto \tilde{M}(\vartheta)$

(3) $\tilde{M}_T(\vartheta) \xrightarrow{a.s.} \tilde{M}(\vartheta)$ uniformly in ϑ as $T, \xi_T = o(\sqrt{T}) \rightarrow \infty$

Finally show that the order of $\|\hat{f}_T - f\|^2$ is that of

$$\left\| \hat{\vartheta}_T - \vartheta_0 \right\| \frac{\xi_T^2}{\sqrt{T}} \frac{1}{\xi_T^2} \sum_{|k| \leq \xi_T} |f_k| |k| |G_k^T|$$

Asymptotic Normality

$0 = \text{grad}_\vartheta \tilde{M}_T(\hat{\vartheta}_T) = \text{grad}_\vartheta \tilde{M}_T(\vartheta_0) + \text{Hess}_\vartheta \tilde{M}_T(\vartheta_0)(\hat{\vartheta}_T - \vartheta_0) + (\text{Hess}_\vartheta \tilde{M}_T(\vartheta^*) - \text{Hess}_\vartheta \tilde{M}_T(\vartheta_0))(\hat{\vartheta}_T - \vartheta_0)$ with

- (1) $\sqrt{T} \text{grad}_\vartheta \tilde{M}_T(\vartheta_0) \xrightarrow{D} \mathcal{N}(0, 16\pi^2\sigma^2\Sigma)$
- (2) $\text{Hess}_\vartheta \tilde{M}_T(\vartheta_0) \xrightarrow{a.s.} 8\pi^2\Sigma$

Asymptotic Normality

Theorem 2

Under $T \rightarrow \infty$, $\xi_T = o(T^{1/4}) \rightarrow \infty$, if $\hat{\vartheta}_T \rightarrow \vartheta_0$ a.s. and

- $f \in H^\rho([0, 1]^2)$ for $\rho = 2$
- $\vartheta \mapsto \delta_t^\vartheta$ is C^2 with uniformly bounded derivatives
- $A_{t,t'}^\vartheta := \text{grad}_\vartheta \langle k, \delta_t^\vartheta \rangle (\text{grad}_\vartheta \langle k, \delta_{t'}^\vartheta \rangle)'$
- $\Sigma := \sum_{k \in \mathbb{Z}^2} |f_k|^2 \left(\int_0^1 A_{t,t}^{\vartheta_0} dt - \iint_{[0,1]^2} A_{t,t'}^{\vartheta_0} dt dt' \right)$

we have

$$\sqrt{T}\Sigma(\hat{\vartheta}_T - \vartheta_0) \xrightarrow{D} \mathcal{N}\left(0, \frac{\sigma^2}{4\pi^2} \Sigma\right).$$

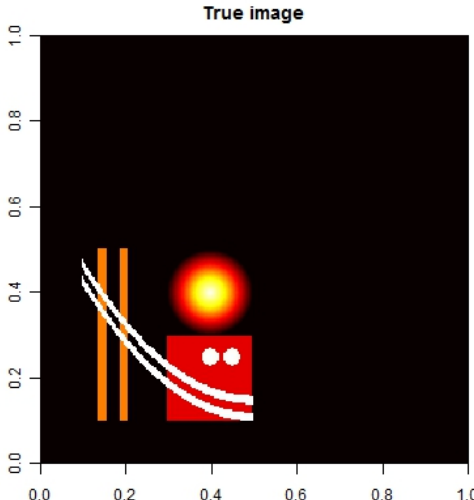
Proof.

$0 = \text{grad}_\vartheta \tilde{M}_T(\hat{\vartheta}_T) = \text{grad}_\vartheta \tilde{M}_T(\vartheta_0) + \text{Hess}_\vartheta \tilde{M}_T(\vartheta_0)(\hat{\vartheta}_T - \vartheta_0) + (\text{Hess}_\vartheta \tilde{M}_T(\vartheta^*) - \text{Hess}_\vartheta \tilde{M}_T(\vartheta_0))(\hat{\vartheta}_T - \vartheta_0)$ with

$$(1) \quad \sqrt{T} \text{grad}_\vartheta \tilde{M}_T(\vartheta_0) \xrightarrow{D} \mathcal{N}(0, 16\pi^2\sigma^2\Sigma)$$

$$(2) \quad \text{Hess}_\vartheta \tilde{M}_T(\vartheta_0) \xrightarrow{\text{a.s.}} 8\pi^2\Sigma$$

Simulations



Test image of about $N = 65,000$ pixels. For $T \in \{20, 50, 100\}$ select in every single frame randomly $n_t = N/T$ pixels. Original noise level $\sigma = 0.25$.

Simulations

Image
Enhancement

Drift Model

Asymptotics

Simulations

Application

Stem Cells

Polarization

SiZer

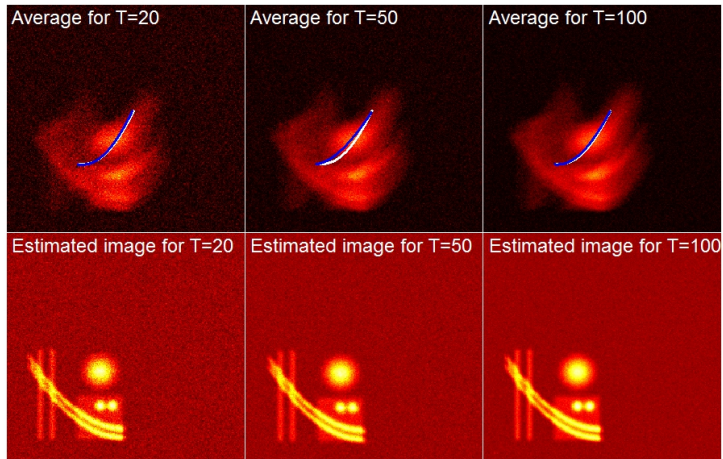
WiZer

Biomechanics

Discussion

References

References



Gauss noise, cubic drift.
White: true drift. Blue: estimated drift.

Simulations

Image
Enhancement

Drift Model

Asymptotics

Simulations

Application

Stem Cells

Polarization

SiZer

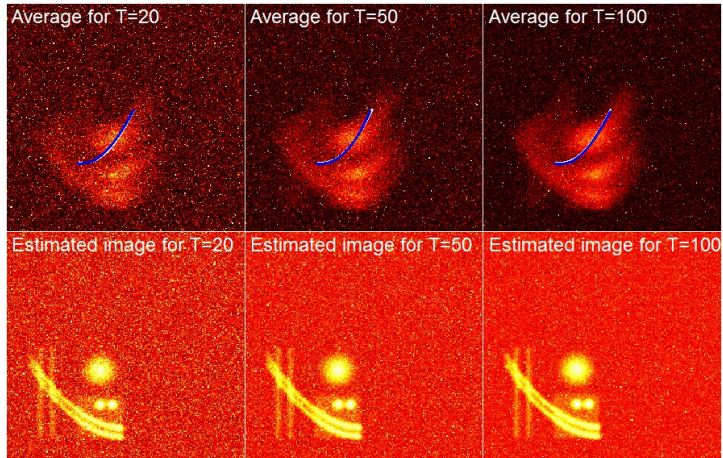
WiZer

Biomechanics

Discussion

References

References



Student t_2 noise, cubic drift.
White: true drift. Blue: estimated drift.

Simulations

Image
Enhancement

Drift Model

Asymptotics

Simulations

Application

Stem Cells

Polarization

SiZer

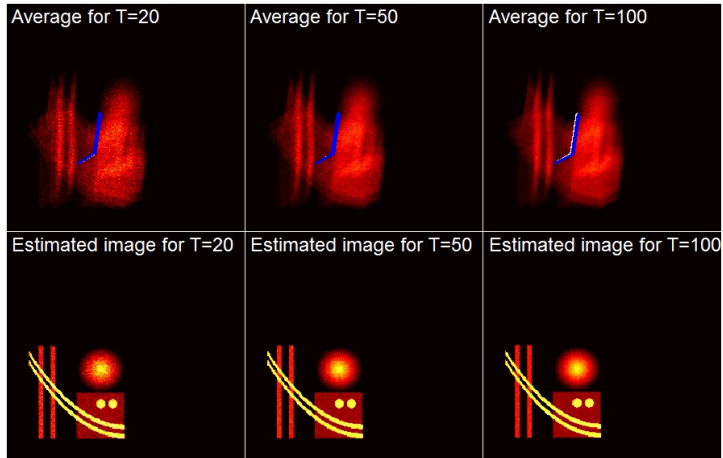
WiZer

Biomechanics

Discussion

References

References

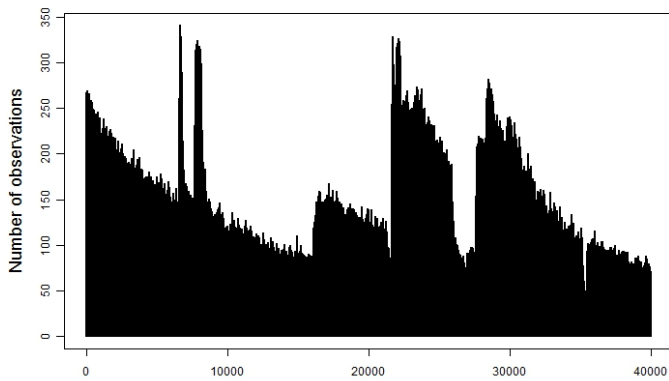


Linear changepoint drift with Poisson noise.
White: true drift. Blue: estimated drift.

Applications to Microtubules-Imaging

RHS-labeled β -tubulin network in a fixed PtK2-cell (male rat kangaroo kidney epithel)

- area: $327 \times 327 \text{ nm}^2$
- frame #: 40,000
- binning: ≈ 100 frames



Stats for Live
Cells

Huckemann

Image
Enhancement

Drift Model

Asymptotics

Simulations

Application

Stem Cells

Polarization

SiZer

WiZer

Biomechanics

Discussion

References

References

Applications to Microtubules-Imaging

First and last single images of PALMIRA data



• • •



Applications in Nanomicroscopy

Image
Enhancement
Drift Model
Asymptotics
Simulations
Application

Stem Cells

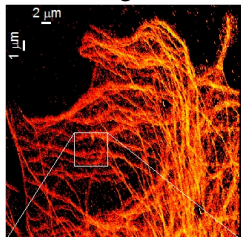
Polarization
SiZer
WiZer
Biomechanics

Discussion

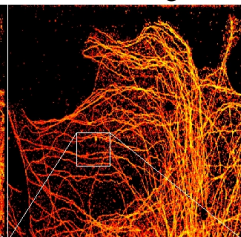
References

References

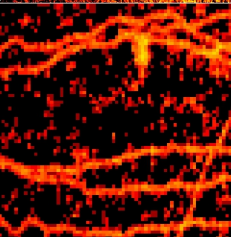
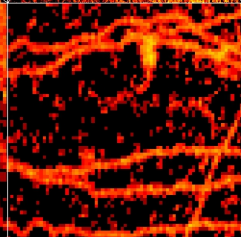
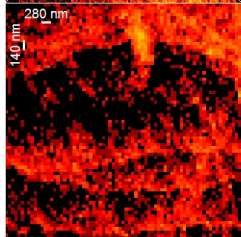
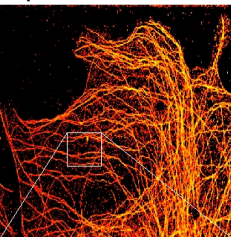
Raw image



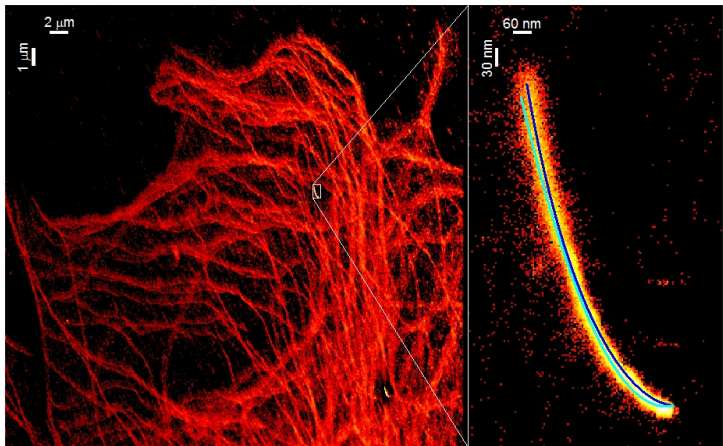
bead tracking



sparse deconvolution



Applications in Nanomicroscopy



Blue: fit to bead drift. Cyan: overall drift

Bootstrap Confidence Bands

Image
Enhancement

Drift Model

Asymptotics

Simulations

Application

Stem Cells

Polarization

SiZer

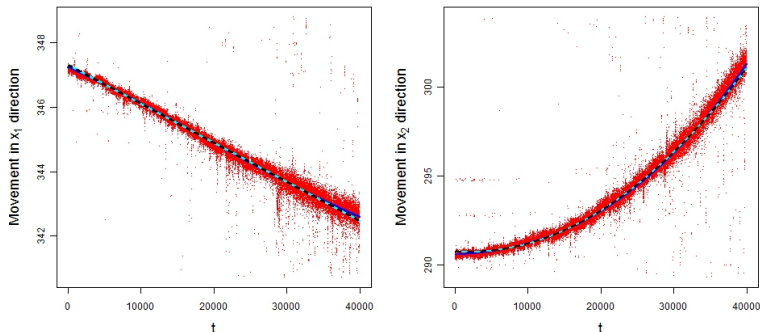
WiZer

Biomechanics

Discussion

References

References

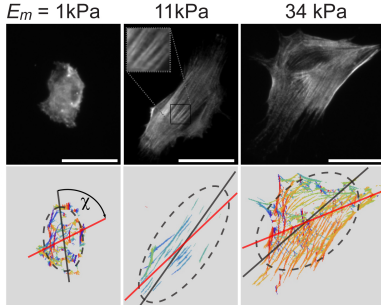


Under the hypothesis of a (low order) polynomial drift, very narrow simultaneous confidence intervals (due to a much larger number of pixel data than of bead data).

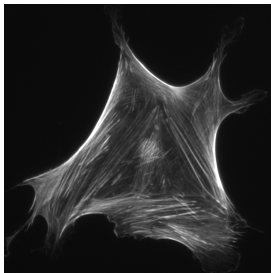
Early Stem Cell Differentiation

- Varying elasticity (kPa),
- soft (neuron, fat, etc.): 1kPa
- medium (muscle) resonance; 11kPa
- hard (bone, scar, etc.): 34 kPa

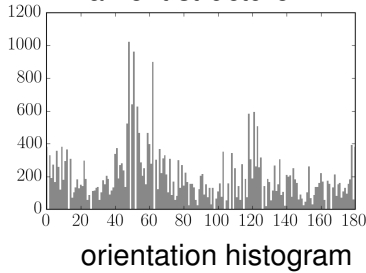
From Zemel et al. (2010)



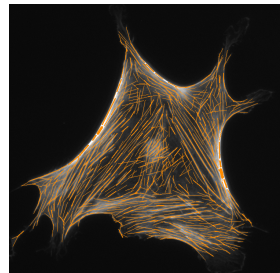
Polarization of Stress Fibres



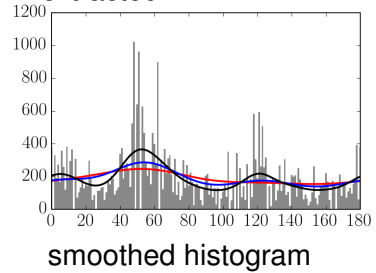
Actin-myosin
filament structure



orientation histogram



linear filaments
extracted



smoothed histogram

The Linear Scale Space / SiZer of Chaudhuri and Marron (1999, 2000)

- Unknown density $f : \mathbb{R} \rightarrow \mathbb{R}^+$,
- f_n its empirical histogram,
- $\hat{f}_n^{(h)} := g^{(h)} * f_n$ its kernel smoothed version,
- $\hat{f}^{(h)} := g^{(h)} * f$ the true kernel smoothed version,
- all with bandwidth $h \in \mathbb{R}^+$.

The Linear Scale Space / SiZer of Chaudhuri and Marron (1999, 2000)

- Unknown density $f : \mathbb{R} \rightarrow \mathbb{R}^+$,
- f_n its empirical histogram,
- $\hat{f}_n^{(h)} := g^{(h)} * f_n$ its kernel smoothed version,
- $\hat{f}^{(h)} := g^{(h)} * f$ the true kernel smoothed version,
- all with bandwidth $h \in \mathbb{R}^+$.
- We have **confidence** that $\hat{f}_n^{(h)}$ has a **mode** “around” $t \in \mathbb{R}$ if $\exists \epsilon_1, \epsilon_2 > 0$ such that

$$\partial_t \hat{f}_n^{(h)}(t + \epsilon_2) < 0 < \partial_t \hat{f}_n^{(h)}(t - \epsilon_1)$$

with **significance**.

The Linear Scale Space / SiZer

- (a) If $(\partial_t \hat{f}_n^{(h)}(t))_{h,t} \rightarrow \partial_t f^{(h)}$ weakly
- obtain asymptotic confidence levels for the number modes of $f^{(h)}(t)$.

The Linear Scale Space / SiZer

- (a) If $(\partial_t \hat{f}_n^{(h)}(t))_{h,t} \rightarrow \partial_t f^{(h)}$ weakly
 - obtain asymptotic confidence levels for the number modes of $f^{(h)}(t)$.
- (b) If **causality** holds, i.e.
$$\#\text{ modes of } f^{(h)} \leq \#\text{ modes of } f^{(h')} \quad \forall h \geq h' > 0$$
 - obtain asymptotic confidence levels for a lower bound for the number modes of $f = f^{(0)}$.

The Linear Scale Space / SiZer

- (a) If $(\partial_t \hat{f}_n^{(h)}(t))_{h,t} \rightarrow \partial_t f^{(h)}$ weakly
- obtain asymptotic confidence levels for the number modes of $f^{(h)}(t)$.
- (b) If **causality** holds, i.e.

$$\#\text{ modes of } f^{(h)} \leq \#\text{ modes of } f^{(h')} \quad \forall h \geq h' > 0$$

- obtain asymptotic confidence levels for a lower bound for the number modes of $f = f^{(0)}$.

Theorem (Chaudhuri and Marron (1999, 2000))

If f is sufficiently regular and $g^{(h)}$ the Gaussian heat kernel then causality holds and

$$\sqrt{n} \left(\partial_t \hat{f}_n^{(h)}(t) - \partial_t \hat{f}^{(h)}(t) \right) \rightarrow (G_h)_t \text{ weakly}$$

with a Gaussian process $(G_h)_t$.

The Circular SiZer

Which smoothing kernel on the circle $[-\pi, \pi)$ gives

- ① empirical scale space tube \rightarrow Gaussian process?
- ② causality of the scale space tube?

\Rightarrow confidence bounds from below for number of true modes.

The Circular SiZer

Which smoothing kernel on the circle $[-\pi, \pi)$ gives

- ① empirical scale space tube \rightarrow Gaussian process?
- ② causality of the scale space tube?

\Rightarrow confidence bounds from below for number of true modes.

- ① Kernels with second moments, e.g. the von Mises density, making the **CircSiZer** by Oliveira et al. (2013):

$$m_\kappa(x) := \frac{1}{2\pi I_0(\kappa)} e^{\kappa \cos(x)}.$$

The Circular SiZer

Which smoothing kernel on the circle $[-\pi, \pi)$ gives

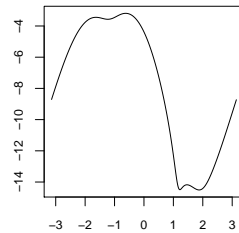
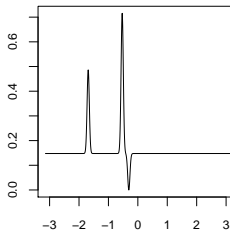
- ① empirical scale space tube \rightarrow Gaussian process?
- ② causality of the scale space tube?

\Rightarrow confidence bounds from below for number of true modes.

- ① Kernels with second moments, e.g. the von Mises density, making the **CircSiZer** by Oliveira et al. (2013):

$$m_\kappa(x) := \frac{1}{2\pi I_0(\kappa)} e^{\kappa \cos(x)}.$$

- ② The **CircSiZer** is not causal (cf. also Munk (1999)):



The Circular SiZer

Which smoothing kernel on the circle $[-\pi, \pi)$ gives

- ① empirical scale space tube \rightarrow Gaussian process?
- ② causality of the scale space tube?

\Rightarrow confidence bounds from below for number of true modes.

- ① Kernels with second moments, e.g. the von Mises density, making the **CircSiZer** by Oliveira et al. (2013):

$$m_\kappa(x) := \frac{1}{2\pi I_0(\kappa)} e^{\kappa \cos(x)}.$$

- ② Theorem 3 (The WiZer)

The solution of the circular heat equation: the wrapped Gaussian

$$g_h^{(w)}(x) := \sum_{m=-\infty}^{\infty} \frac{1}{\sqrt{2\pi} h} e^{-\frac{(x+2\pi m)^2}{2h^2}}.$$

guarantees causality of the scale space tube.

Circular Scale Space Axiomatics

A family $\{L_h : h > 0\}$ of convolution kernels ($\int L_h = 1$) is

- a **semi-group** if $L_{h+h'} = L_h * L_{h'}$ for all $h, h' > 0$
- **causal** if $S(L_h * f) \leq S(f)$ for all f
- **strongly Lipschitz** if $\exists r > 0$

$\forall \epsilon > 0 \ \exists h_0 = h_0(\epsilon) > 0$ such that $|(\mathcal{F}L_h)_k - 1| < \epsilon h |k|^r$

for all $k \in \mathbb{Z}$ and all $0 < h \leq h_0$.

Circular Scale Space Axiomatics

A family $\{L_h : h > 0\}$ of convolution kernels ($\int L_h = 1$) is

- a **semi-group** if $L_{h+h'} = L_h * L_{h'}$ for all $h, h' > 0$
- **causal** if $S(L_h * f) \leq S(f)$ for all f
- **strongly Lipschitz** if $\exists r > 0$

$\forall \epsilon > 0 \ \exists h_0 = h_0(\epsilon) > 0$ such that $|(\mathcal{F}L_h)_k - 1| < \epsilon h |k|^r$

for all $k \in \mathbb{Z}$ and all $0 < h \leq h_0$.

Theorem 4

The only causal and strongly Lipschitz semi-group on the circle is given by the wrapped Gaussians.

For Euclidean analogs, e.g. Weickert et al. (1999);
Lindeberg (2011).

Persistence of Modes

- Scale spaces allow for definition of persistences:
- WiZer (SiZer) requires a smallest bandwidth (Schmidt-Hieber et al. (2013) does not),
- coming from the other side (large to small bandwidth),
- at some bandwidth the first mode pops up
- persists until the second pops up
- persists until the third ...
- ...

Log Persistences: Boxplots

Image
Enhancement

Drift Model

Asymptotics

Simulations

Application

Stem Cells

Polarization

SiZer

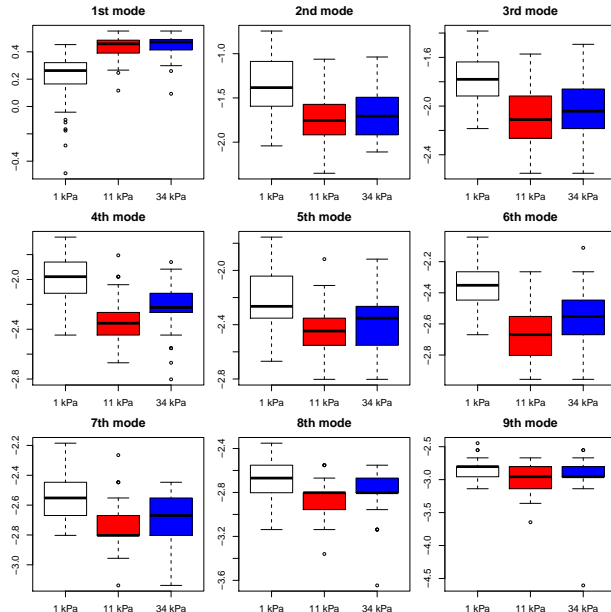
WiZer

Biomechanics

Discussion

References

References



Discussion

- Stochastic switching gives arbitrary precision with increased sparsity,

Discussion

- Stochastic switching gives arbitrary precision with increased sparsity,
- WiZer (circular scale space theory) and persistence diagrams,
- early environment's elasticity links to biological function.

Discussion

- Stochastic switching gives arbitrary precision with increased sparsity,
- WiZer (circular scale space theory) and persistence diagrams,
- early environment's elasticity links to biological function.

References

- Abbe, E. (1873). Beiträge zur Theorie des Mikroskops und der mikroskopischen Wahrnehmung. *Archiv für mikroskopische Anatomie* 9(1), 413–418.
- Betzig, E., G. H. Patterson, R. Sougrat, O. W. Lindwasser, S. Olenych, J. S. Bonifacino, M. W. Davidson, J. Lippincott-Schwartz, and H. F. Hess (2006). Imaging intracellular fluorescent proteins at nanometer resolution. *Science* 313(5793), 1642–1645.
- Brown, L. D., I. M. Johnstone, and K. B. MacGibbon (1981). Variation diminishing transformations: A direct approach to total positivity and its statistical applications. *Journal of the American Statistical Association* 76(376), 824–832.
- Chaudhuri, P. and J. Marron (1999). Sizer for exploration of structures in curves. *Journal of the American Statistical Association* 94(447), 807–823.
- Chaudhuri, P. and J. Marron (2000). Scale space view of curve estimation. *The Annals of Statistics* 28(2), 408–428.
- Egner, A., C. Geisler, C. von Middendorff, H. Bock, D. Wenzel, R. Medda, M. Andresen, A. Stiel, S. Jakobs, C. Eggeling, A. Schoenle, and S. W. Hell (2007). Fluorescence nanoscopy in whole cells by asynchronous localization of photoswitching emitters. *Biophysical Journal* 93, 3285–3290.
- Geisler, C., H. T., A. Schoenle, S. W. Hell, A. Munk, , and A. Egner (2012). Drift estimation for single marker switching based imaging schemes. *Optics Express* 20(7), 7274–7289.
- Hartmann, A., S. Huckemann, J. Dannemann, O. Laitenberger, C. Geisler, A. Egner, and A. Munk (2015). Drift estimation in sparse sequential dynamic imaging: with application to nanoscale fluorescence microscopy. *Journal of the Royal Statistical Society, Series B*. early online access.
- Hell, S. W. (2007). Far-field optical nanoscopy. *Science* 316, 1153–1158.
- Huckemann, S. F., K.-R. Kim, A. Munk, F. Rehfeld, M. Sommerfeld, J. Weickert, and C. Wollnik (2015). The circular sizer, inferred persistence of shape parameters and application to stem cell stress fibre structures. *Bernoulli*. early online access.
- Lindeberg, T. (2011). Generalized gaussian scale-space axiomatics comprising linear scale-space, affine scale-space and spatio-temporal scale-space. *Journal of Mathematical Imaging and Vision* 40(1), 36–81.
- Mairhuber, J., I. Schoenberg, and R. Williamson (1959). On variation diminishing transformations on the circle. *Rendiconti del Circolo matematico di Palermo* 8(3), 241–270.
- Munk, A. (1999). Optimal inference for circular variation diminishing experiments with applications to the von-mises distribution and the fisher-efron parabola model. *Metrika* 50(1), 1–17.
- Oliveira, M., R. M. Crujeiras, and A. Rodríguez-Casal (2013). Circsizer: an exploratory tool for circular data. *Environmental and Ecological Statistics*, 1–17.
- Rust, M. J., M. Bates, and X. W. Zhuang (2006). Sub-diffraction-limit imaging by stochastic optical reconstruction microscopy (storm). *Nature Methods* 3, 793–795.

References

- Schmidt-Hieber, J., A. Munk, and L. Dümbgen (2013). Multiscale methods for shape constraints in deconvolution: Confidence statements for qualitative features. *Ann. Statist.* 41(3), 1299–1328.
- Weickert, J., S. Ishikawa, and A. Imiya (1999). Linear scale-space has first been proposed in Japan. *Journal of Mathematical Imaging and Vision* 10(3), 237–252.
- Zemel, A., F. Rehfeldt, A. E. X. Brown, D. E. Discher, and S. A. Safran (2010). Optimal matrix rigidity for stress-fibre polarization in stem cells. *Nat Phys* 6(6), 468–473.